Int. J. Solids Structures Vol. 27, No. 1, pp. 1–14, 1991
Printed in Great Britain.

0020–7683/91 $3.00+.00

ON THE RESPONSE AND STABILITY OF TWO CONCENTRIC, CONTACTING RINGS UNDER EXTERNAL PRESSURE

F.-S. LI and S. KYRIAKIDES
Engineering Mechanics Research Laboratory, Department of Aerospace Engineering and Engineering Mechanics, The University of Texas at Austin, TX 78712, U.S.A.

(*Received* 31 *May* 1989; *in revised form* 24 *October* 1989)

Abstract—The problem considered involves two concentric, smoothly contacting rings under external pressure. The outer ring is initially circular but the inner ring has a localized initial imperfection which causes a small section of the ring to be detached from the outer one. The pressure is applied externally but also in the cavity formed by the imperfection. The formulation used is general enough to allow for large deflections. The material of both rings is assumed to be linearly elastic. The nonlinear response of the structure was found to be characterized by a limit load type of instability. The mode of collapse and the limit load are shown to depend on the geometric characteristics of the two rings and those of the initial imperfection.

INTRODUCTION

This paper deals with the response and stability of two concentric, smoothly contacting, thin, elastic rings under external pressure. The outer ring is circular but the inner one has a small localized imperfection as shown in Fig. 1. The pressure is applied to the outer ring as well as in the cavity formed by the imperfection. The main objective of this study is to illustrate how the presence of the outer ring increases the capacity of the inner one to resist collapse and also how the mechanism of instability and the post buckling response are altered.

The particular pressure loading adopted and the type of imperfections used are ones which approximately represent those encountered in the situation of a propagating buckle engaging a slip-on buckle arrestor described by Kyriakides and Babcock (1980). Similar conditions were also described in the problem of a propagating buckle which can affect long cylindrical shells used as liners for relatively stiff cylindrical cavities (see Kyriakides, 1986).

The complexity of the problem can be appreciated by reviewing a series of published studies dealing with the response and stability of rings confined in rigid contacting cavities. Among others, Pian and Bucciarelli (1967) and Zagustin and Herrmann (1967) considered a confined ring loaded by a uniform parallel load. Bucciarelli and Pian (1967) and El-Bayoumi (1972) considered the same geometry under thermal loading. Kyriakides and Youn (1984) and Yamamoto and Matsubara (1981) addressed similar problems but under pressure loading. More recently Bottega (1988) addressed the case of a confined ring acted upon by a point radial load. The main conclusions from these studies are that the ring has a very stiff prebuckling response which is characterized by a limit load and that the limit load is strongly influenced by initial geometric imperfections.

This study differs from these works in that it considers the confining structure to be a deformable ring. The problem is formulated and solved through beam kinematics which allow for large deflections but shear deformations are neglected. The problem is solved numerically and the prebuckling and large deflection postbuckling responses are calculated.

PROBLEM FORMULATION

We consider two concentric, thin-walled, smoothly contacting rings of radius R and wall thicknesses t_0 for the outside and t_i for the inside ring. The inside ring has a small initial geometric imperfection which causes a length of $2\hat{s}$ to be detached from the outer ring as shown in Fig. 1. The imperfection is generated numerically through a process

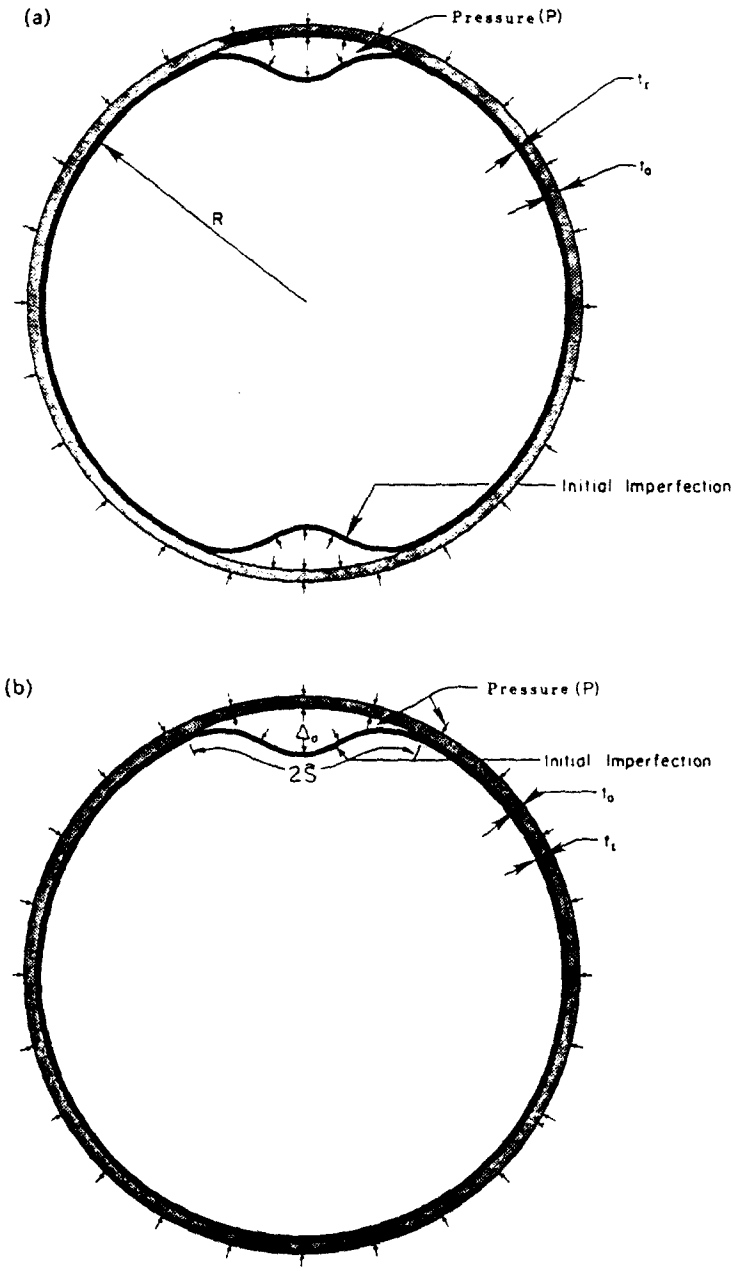

Fig. 1. Problem geometry. (a) Doubly symmetric case. (b) Singly symmetric case.

described in the next section. Relative to the rectangular coordinate system (x–y), shown in Fig. 2, the imperfection geometry is defined through

$$\hat{x} = \hat{x}(s, \Delta_0), \quad \hat{y} = \hat{y}(s, \Delta_0) \quad \text{and} \quad \hat{\theta} = \hat{\theta}(s, \Delta_0), \tag{1}$$

where Δ_0 is the initial amplitude of the imperfection crown point which is a prescribed parameter [$\Delta_0 = R - \hat{x}(0, \Delta_0)$]. The imperfection is symmetric about $y = 0$.

The two rings are pressurized externally with hydrostatic pressure P which is also applied in the cavity formed between them due to the initial geometric imperfection. We seek to establish the response of the assembly due to the applied external pressure.

Two cases are considered; the first, shown in Fig. 1a, has two planes of symmetry and the second, shown in Fig. 1b, has one plane of symmetry. It is assumed that during deformation the respective symmetries are maintained.

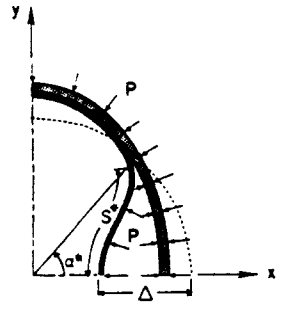

Fig. 2a. Deformed geometry of doubly symmetric case.

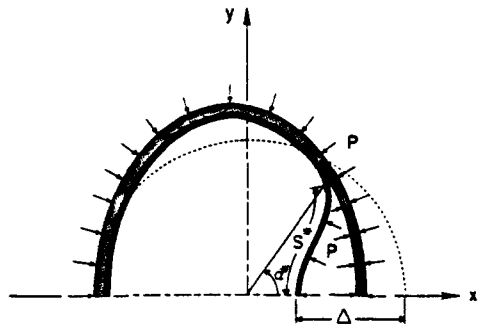

Fig. 2b. Deformed geometry of singly symmetric case.

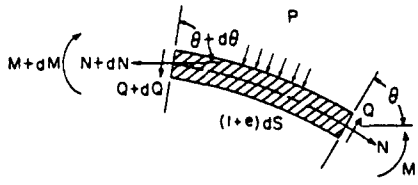

Fig. 2c. Equilibrium of forces of ring element.

The problem is formulated through a class of small strain but finite rotation kinematics (see Reissner, 1972) in which the transverse shear deformations are neglected as is customary in the analysis of thin-walled structures. In addition to nonlinear kinematics the nonlinearity of changing contact length between the two rings must be addressed. In what follows the formulation for the doubly symmetric case is discussed in detail followed by a brief discussion of the main difference of this formulation from that of the singly symmetric case.

We identify the point of separation of the two rings by the angle α^* and the detached length by s^* as shown in Fig. 2. We define the current configuration by the coordinates (x, y), of the respective ring mid-surface, and by the angle θ between the normal to the ring mid-surface and the x-axis.

The axial force intensity N, the shear force intensity Q and the bending moment intensity M acting on the cross-sections of the rings are defined (positive sense) in Fig. 2c (for convenience we assume the two rings to have unit width).

In the analysis the two rings are separated as shown in Fig. 3 and the variables are identified by the subscript "O" for the outside ring and "I" for the inside ring. Based on

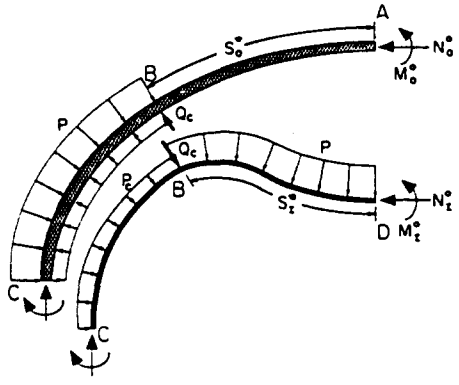

Fig. 3. Free body diagram of two rings.

the above, the field equations for the two rings can be expressed as follows:

$$\begin{aligned}
&\frac{dx_i}{ds_i} = -(1+e_i)\sin\theta_i,\\
&\frac{dy_i}{ds_i} = (1+e_i)\cos\theta_i, \qquad i = O, I\\
&\frac{d\theta_i}{ds_i} = \frac{d\bar{\theta}_i}{ds_i} - \kappa_i, \qquad 0 \leqslant s_i \leqslant \frac{\pi R}{2}\\
&\frac{dN_i}{ds_i} = Q_i\frac{d\theta_i}{ds_i},\\
&\frac{dQ_i}{ds_i} = -\frac{d\theta_i}{ds_i}N_i - (1+e_i)P_i,\\
&\frac{dM_i}{ds_i} = (1+e_i)Q_i.
\end{aligned} \tag{2}$$

e and κ represent the membrane and bending strains in the rings and s is a measure of length along the undeformed ring mid-surface. $d\bar{\theta}/ds$ is the initial curvature. It has a value of $1/R$ except in the region of the imperfection where the value is obtained from (1). As a first step we assume both rings to be linearly elastic (moduli E_i). As a result the following constitutive equations are appropriate:

$$\begin{aligned}
&N_i = E_i t_i e_i,\\
&M_i = E_i\frac{t_i^3}{12}\kappa_i. \qquad i = O, I.
\end{aligned} \tag{3}$$

For analytical convenience the structure is separated into three sections, AB, BC and DB identified in the free body diagram shown in Fig. 3. Equations (2) and (3) are used to analyze each section. For section AB $P_O = 0$ and for section DB $P_I = P$. BC is the section over which the two rings are in contact. A contact pressure, $P_c(s_O)$, develops between the two rings in this section. In addition a concentrated contact force Q_c develops between the two rings at the point of separation B.

Over the section of contact the two rings have the same displacements (i.e. same x, y and θ) and the same curvature. As a result

$$M_O(s_O) = mM_I(s_I), \qquad s_i^* \leqslant s_i \leqslant \frac{\pi R}{2}, \tag{4}$$

and

$$Q_O(s_O) = mQ_I(s_I), \tag{5}$$

where

$$m = \frac{E_O t_O^3}{E_I t_I^3}.$$

Simple manipulations of eqns (1) lead to the following expression for the contact pressure P_c:

$$P_c(s_O) = \frac{1}{(1+e_O)(1+m)}\left[(1+e_O)P + \frac{d\theta_O}{ds_O}(N_O - mN_I)\right], \quad s_O^* \leqslant s_O \leqslant \frac{\pi R}{2}, \tag{6}$$

where

$$N_I(s_O) = \frac{1}{m}[N_O(s_O) + mN_I(s_I^*) - N_O(s_O^*)]. \tag{7}$$

The point shear force Q_c acting at B can be expressed in terms of other variables as follows:

$$Q_c = \frac{1}{(1+m)}\{N_O^0 \sin\theta^* - m[N_I^0 \sin\theta^* + P[y_I^* \cos\theta^* + (x_I^0 - x_I^*)\sin\theta^*]]\} \tag{8}$$

where the superscript $(\,)^0$ refers to values at $s_i = 0$ and the superscript $(\,)^*$ refers to values at $s_i = s_i^*$.

Thus for the section BC P_O in (2) is given by $P_O = P - P_c(s_O)$. Once the solution for the outer ring is known the variables M_I, N_I, Q_I, and e_I can be obtained from (4), (7), (5) and (3).

Boundary conditions

For the outer ring:

$$y_O(0) = 0, \quad \theta_O(0) = 0, \quad Q_O(0) = 0, \quad x_O\left(\frac{\pi R}{2}\right) = 0, \quad \theta_O\left(\frac{\pi R}{2}\right) = \frac{\pi}{2}, \quad Q_O\left(\frac{\pi R}{2}\right) = 0. \tag{9}$$

Because this section is analyzed in two parts (AB and BC) at $s_O = s_O^*$ we require continuity of x_O, y_O, θ_O, N_O and M_O. The shear experiences a jump due to the presence of the concentrated force Q_c. Thus

$$Q_O(s_O^{*-}) = Q_O(s_O^{*+}) - Q_c. \tag{10}$$

For the inner ring:

$$x_I(0) = R - \Delta, \quad y_I(0) = 0, \quad \theta_I(0) = 0, \quad Q_I(0) = 0 \tag{11a}$$

where Δ will be the prescribed variable in the incremental solution procedure we will adopt. At point B the contact condition requires that

$$x_I(s_I^*) = x_O(s_O^*), \quad y_I(s_I^*) = y_O(s_O^*), \quad \theta_I(s_I^*) = \theta_O(s_O^*) \tag{11b}$$

and

$$M_I(s_I^*) = \frac{1}{m} M_O(s_O^*).$$

s_I^* and s_O^* are related as follows:

$$s_O^* - \int_{s_O^*}^{\pi R/2} e_O \, ds_O = s_I^* - \int_{s_I^*}^{\pi R/2} e_I \, ds_I. \tag{12}$$

The membrane strain e_I for this section can be obtained from (3) and (7).

The problem with the single plane of symmetry (Fig. 1b) can be analyzed through the same equations by changing the domain of s_O to

$$s_O^* \leqslant s_O \leqslant \pi R.$$

The boundary conditions at $s_0 = \pi R$ become

$$y_O(\pi R) = 0, \quad \theta_O(\pi R) = \pi \quad \text{and} \quad Q_O(\pi R) = 0. \tag{13}$$

In the numerical analysis of this problem the point $s_O = \pi R$ was kept fixed thus in addition to (13) $x_O(\pi R) = -R$.

Initial imperfection

For cases in which the outer ring is rigid, the response and stability of the inner ring were shown to be strongly influenced by the presence of small initial localized geometric imperfections (see Kyriakides and Youn, 1984 for pressure loading; Bucciarelli and Pian, 1967 for thermal loading). Motivated by these results, and by the practical aspects of the buckle arrestor problem mentioned in the Introduction, a localized initial imperfection was introduced to the problem in the fashion shown in Figs 1a and 1b. The geometry of the imperfection was obtained by solving the following special case of the problem. The outer ring was assumed to be rigid and the inner ring to be inextensional and in perfect smooth contact with the outer ring. A sequence of buckled configurations were obtained numerically following the procedure described by Kyriakides and Youn (1984). Such a sequence of configurations and the corresponding pressure-detached length responses are shown in Fig. 4.

Such configurations with relatively small values of crown displacement (Δ_0) and assumed to be initially unstressed were used in the analysis presented as initial imperfections by representing their geometry through $\{\hat{x}(s_1, \Delta_0), \hat{y}(s_1, \Delta_0), \hat{\theta}(s_1, \Delta_0)\}$.

Numerical solution

The nonlinear differential equations for sections AB, BC and DB with the appropriate boundary conditions were solved numerically. The differential equations were discretized

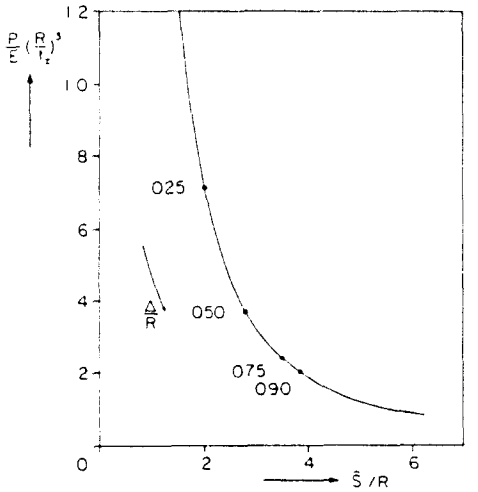

Fig. 4a. Pressure-detached length response of initially perfect ring in a rigid cavity.

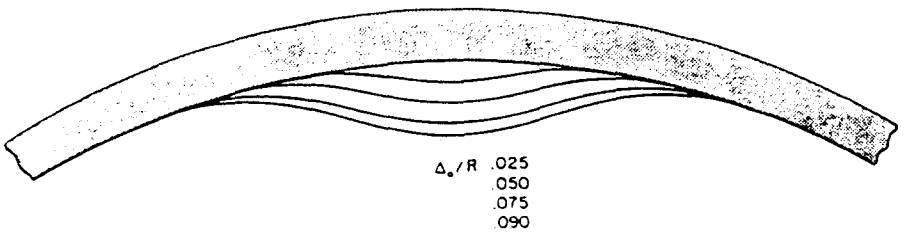

Fig. 4b. Deformed configurations corresponding to crown displacements indicated in Fig. 4a.

through a forward difference scheme which involved I, J and K difference intervals for AB, BC and DB, respectively. The discretization lead to $6(I+J+K)$ nonlinear algebraic equations. The compatibility relationship (12) was added to this assemblage.

The nonlinear equations were solved iteratively using the Levenberg–Marquardt algorithm as modified by Powell (1970). For a system of nonlinear algebraic equations $\mathbf{f}(\mathbf{x}) = \boldsymbol{\phi}$ the algorithm is given by

$$\mathbf{x}_{n+1} = \mathbf{x}_n - [\lambda_n \mathbf{I} + \mathbf{J}_n^T \mathbf{J}_n]^{-1} \mathbf{J}_n^T \mathbf{f}(\mathbf{x}_n)$$

where

$$\mathbf{J}_n = \frac{\partial \mathbf{f}}{\partial \mathbf{x}}(\mathbf{x}_n),$$

$\mathbf{x}_n$ is the current, known, approximate value for the unknown vector $\mathbf{x}$ and λ_n is a scalar.

Unlike Newton's method, this particular algorithm allows the use of an initial guess to the solution, $\mathbf{x}_1$, which is not required to be close to the actual solution $\mathbf{x}$. The algorithm is a combination of the method of *steepest descent* and *Newton's method*. The first converges linearly but can work even with a relatively bad initial guess. The second converges quadratically but requires a good initial guess. Thus, by choosing the value of λ_n judiciously the user can use primarily the method of steepest descent initially and primarily Newton's method closer to the solution. A methodology for selecting λ_n is described by Powell (1970).

One of the major challenges of this class of problems is the treatment of the changing domain for the three sets of differential equations (contact problem). This was addressed by letting the length of the three sectors adjacent to point B in the difference scheme be unknown. In addition the pressure loading P was left unknown and the crown displacement, Δ, of the inside ring was prescribed incrementally. If, after convergence, the lengths of these sectors are found to be "large" then another sector is generated by adding one more difference point. If their lengths are found to be "small" then the domain is decreased by subtracting a point. This scheme was found to lead to smaller discretization errors and to efficient execution.

In the formulation presented, a constant pressure P was assumed to act in the cavity formed by the initial imperfection and the outer ring. It was found that pressure loading could only be supported if the initial length over which it was applied was larger than the domain of the cavity prescribed through (1). This type of behavior was also observed for other loads in the works of Pian and Bucciarelli (1967), Zagustin and Herrmann (1967) and Bottega (1988). This problem can be treated by allowing enough flexibility in the numerical algorithm so as to allow the required change in the problem domain. However, the correct detached length of the initial configuration can also be found from a small deflection analysis.

RESULTS AND DISCUSSION

The major characteristics of the problem can be illustrated through an example. The two rings are assumed to have the same Young's modulus, E, and the ratio of their thickness is assumed to be $t_0/t_1 = \sqrt[3]{3}$ and $R/t_1 = 17.9$. The geometric imperfection used had an amplitude of $\Delta_0 = 0.075R$. Both the doubly symmetric as well as the singly symmetric cases were considered. Figures 5a and 5b show sequences of calculated equilibrium configurations for the two cases. Equilibrium configurations up to the one in which the crown point touches the opposite wall were calculated for these cases.

Figure 6a shows a plot of the pressure as a function of the crown displacement, and Fig. 6b shows a plot of the pressure against the detached length. (All variables are suitably normalized.) Clearly the structure is characterized by a limit load instability. The maximum

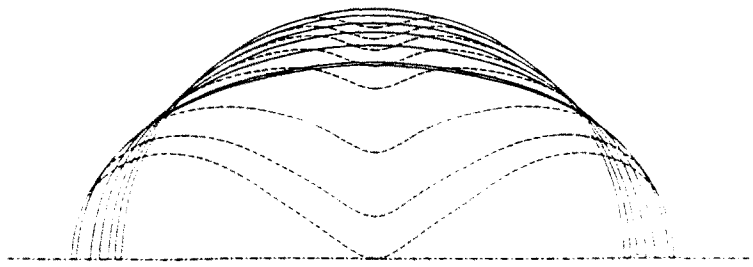

Fig. 5a. Sequence of calculated response configurations for doubly symmetric case $[(t_o/t_i)^3 = 3]$.

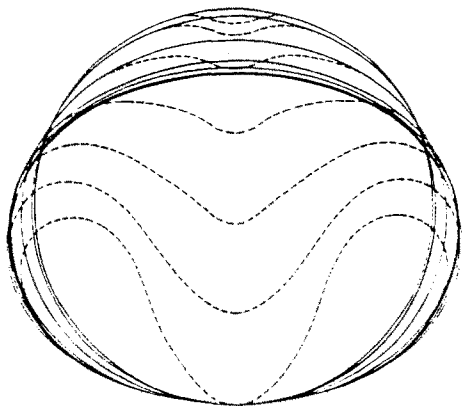

Fig. 5b. Sequence of calculated response configurations for singly symmetric case $[(t_o/t_i)^3 = 3]$.

pressures (P_L) reached in the two cases are as follows:

	$\frac{P_L}{E}\left(\frac{R}{t_i}\right)^3$	$\frac{P_m}{E}\left(\frac{R}{t_i}\right)^3$
Singly symmetric case	0.67	0.33
Doubly symmetric case	0.62	0.36

Thus, in this case the structure has the tendency to deform and collapse in the doubly symmetric mode. Following the limit load, the structure experiences a sharp drop in the load-bearing capacity. The minimum pressures P_m, reached in the postbuckling regime, are also given above. The buckling pressure (normalized) of the inner ring without the reinforcement of the outer one is 0.25; thus the beneficial effect of the outer ring on the stability of the inner one is obvious.

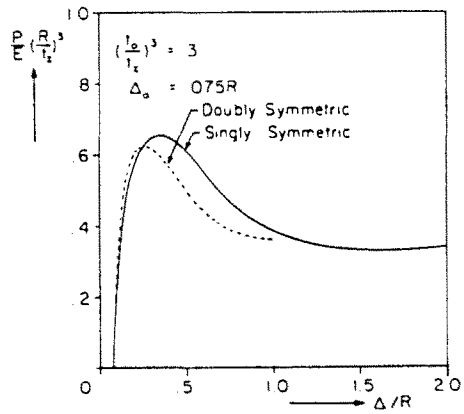

Fig. 6a. Pressure-crown displacement response.

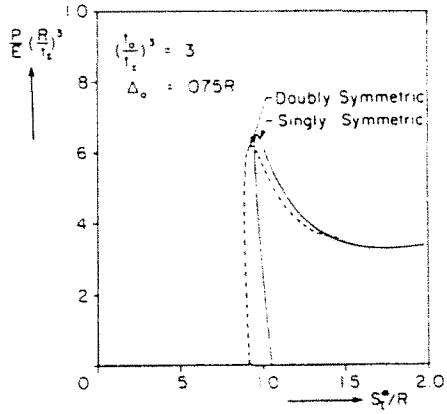

Fig. 6b. Pressure-detached length response.

The crown displacement monotonically increases during the whole process. It was thus a suitable variable for controlling the incremental solution procedure used. By contrast, the detached length decreases for most of the prebuckling part of the response. Close to the limit load it starts increasing with pressure and continues to increase monotonically following the maximum pressure. The characteristics described above are common to both the singly and doubly symmetric cases.

The initial detached length of the imperfection used can be found from Fig. 4a to be $\hat{s}/R = 0.349$. The initial detached lengths acceptable to the solution procedure used were $s_1^*/R = 1.045$ and 0.912 for the singly and double symmetric cases, respectively, which demonstrates the initial jump in s_1^* exhibited by the solution and mentioned in the previous section.

Figure 7 shows plots of the point contact force, Q_c, which develops between the two rings at the point of separation B (see Fig. 3). Figure 8 shows the distribution of the contact pressure P_c over the length for which the two rings are in contact for different values of the crown displacement Δ (doubly symmetric case). At the early stages of deformation, when the section in contact has nearly constant curvature, P_c varies by a very small amount over

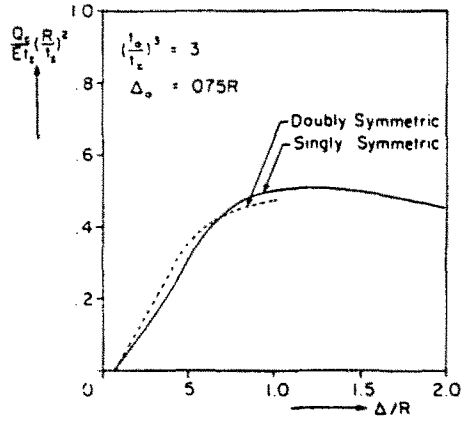

Fig. 7. Contact force at separation point as a function of crown displacement.

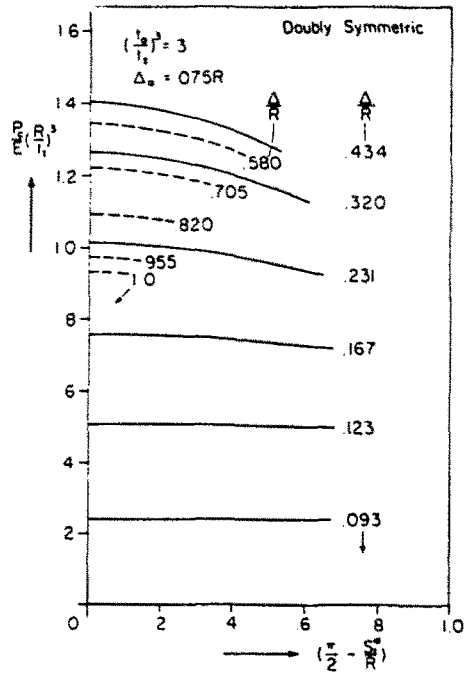

Fig. 8. Contact pressure between two rings for different values of drown displacement.

the length. At the latter stages of deformation the curvature of this section varies over the length; this produces some variation in P_c over the length in contact.

The response of the composite structure is strongly influenced by the stiffness of the outer ring. This is demonstrated in Figs 9a and 9b where the pressure-crown displacement and pressure-detached length responses are plotted for various thickness ratios (t_O/t_I) for the doubly symmetric case. The initial imperfection used again had an amplitude of $\Delta_0/R = 0.075$. The value of the limit load is seen to strongly increase with t_O/t_I. In the case of $t_O/t_I = \sqrt[3]{10^4}$ the outer ring can be viewed to be almost rigid compared to the inner one. Thus the corresponding limit pressure is the highest possible for this imperfection. As the thickness ratio decreases the maximum pressure is reduced. In addition, the prebuckling as well as the postbuckling responses have smaller absolute slope. When the ratio of t_O/t_I is small the responses do not have a limit load as for example $t_O/t_I = 0.4$. This is reminiscent of the response of a single ring under external pressure. The outer ring does, however, still have a stiffening effect as can be seen by comparing the case of $t_O/t_I = 0.4$ and the case with $t_O = 0$.

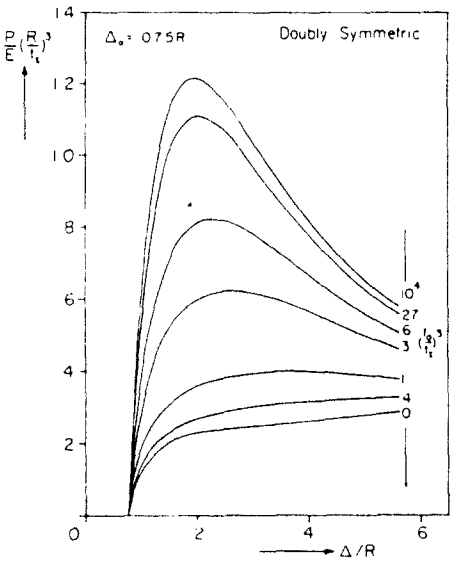

Fig. 9a. Pressure-crown displacement responses for various ring thickness ratios.

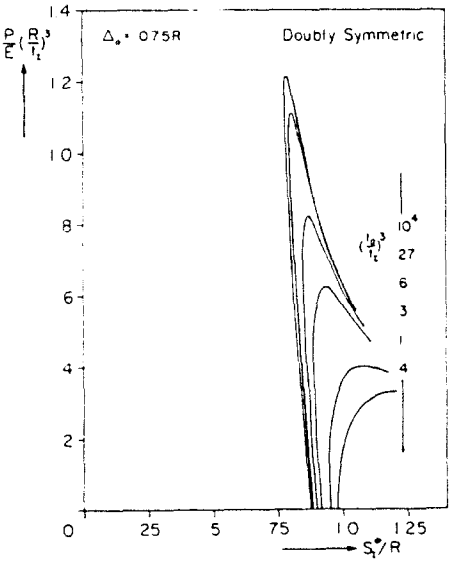

Fig. 9b. Pressure-detached length responses for various ring thickness ratios.

The main features of the responses shown in Fig. 9 are the same as those of the case with $t_O/t_I = \sqrt[3]{3}$ described earlier. However we observe that the initial jump in detached length (difference between $\hat{s}$ and s_I^* at $P = 0$) depends on the ratio of t_O/t_I.

The same geometries were reconsidered through the singly symmetric formulation. The results are shown in Figs 10a and 10b. The main features of these responses are similar to those presented in Fig. 9. However the limit loads obtained for the two cases are different. This difference is demonstrated more clearly in Fig. 11 where the calculated limit pressure P_L is plotted against t_O/t_I for the two cases. For $t_O/t_I > 2.5$ the limit loads from the singly symmetric formulation are lower. For $t_O/t_I < 2.5$ the converse is true. It is thus concluded that for lower values of t_O/t_I the composite structure will deform and collapse in the doubly symmetric mode shown in Fig. 5a. For high values of t_O/t_I the structure will follow the singly symmetric collapse mode as shown in Fig. 5b. It is expected that the value of the transition thickness ratio depends also on the imperfection amplitude.

The effect of the imperfection amplitude Δ_0 on the calculated response is shown in Fig. 12a and 12b. Smaller values of Δ_0 result in stiffer responses with higher limit loads. In

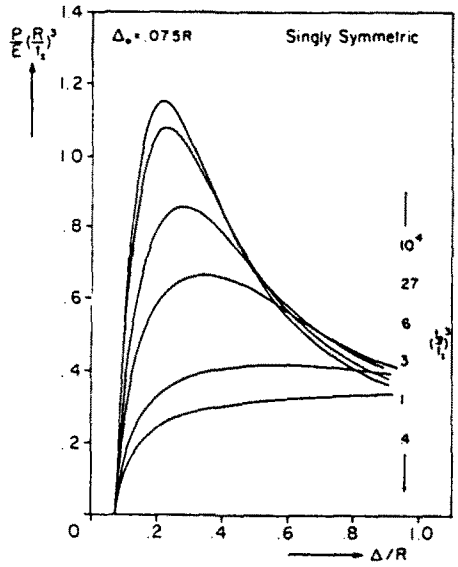

Fig. 10a. Pressure-crown displacement responses for various ring thickness ratios.

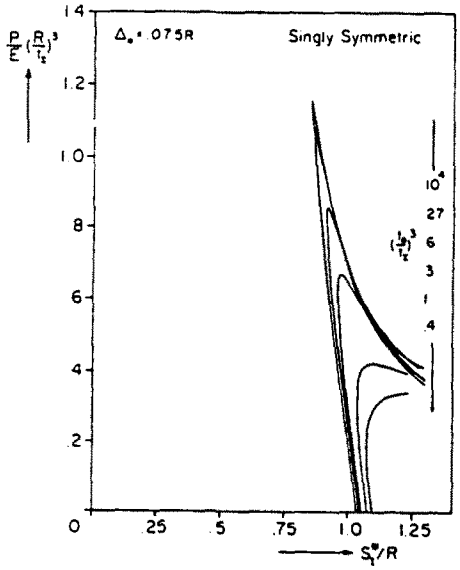

Fig. 10b. Pressure-detached length responses for various ring thickness ratios.

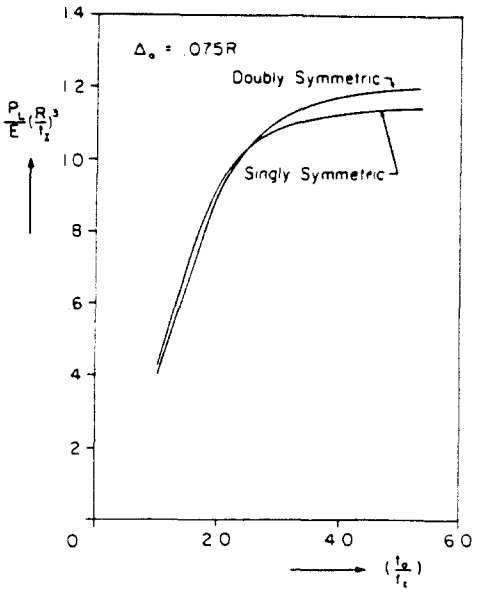

Fig. 11. Limit pressure as a function of ring thickness ratio.

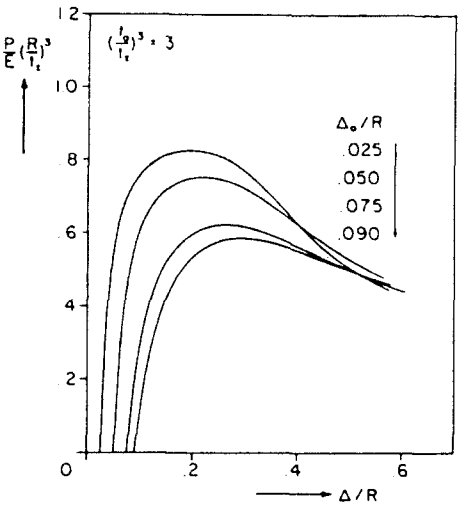

Fig. 12a. Pressure-crown displacement responses for various imperfection amplitudes.

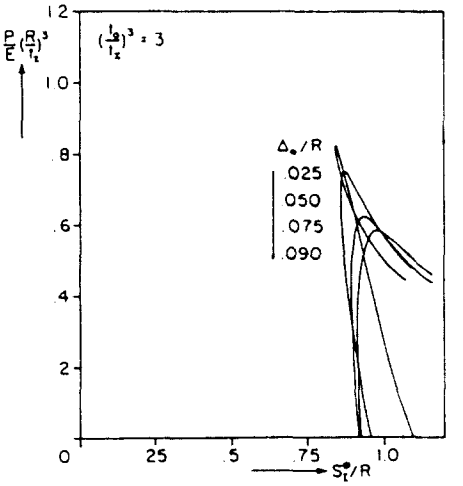

Fig. 12b. Pressure-detached length responses for various imperfection amplitudes.

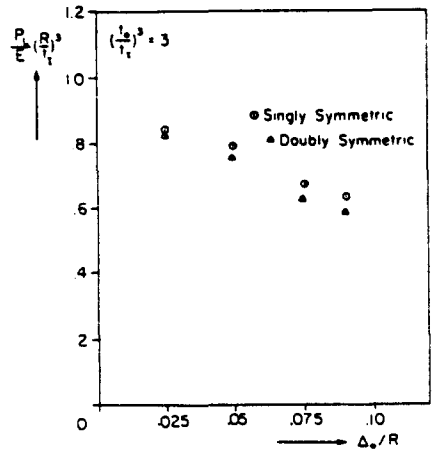

Fig. 13. Limit pressure as a function of imperfection amplitude.

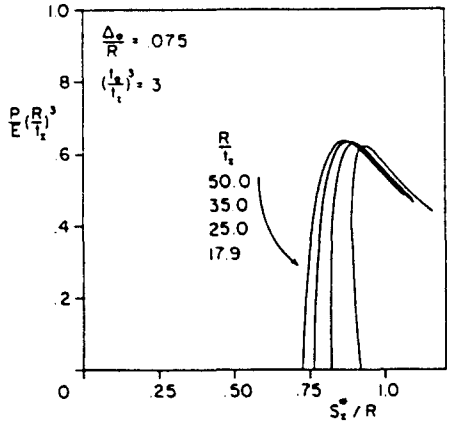

Fig. 14. Pressure-detached length responses for various R/t_1 ratios.

addition, the slope of the prebuckling part of the pressure-detached length response changes drastically with Δ_0 as demonstrated in Fig. 12b. For very small values of Δ_0 the response is seen to develop an unusual loop. The values of the limit loads obtained for different initial imperfection amplitudes for the doubly and singly symmetric cases are compared in Fig. 13. The latter yields consistently higher limit pressures. However, we observe that the difference between the two sets of results decreases for smaller values of Δ_0.

Some insight as to the effect of axial rigidity of the inner ring on the observed response can be obtained from the results shown in Fig. 14. The pressure-detached length response for various R/t_1 values are shown. The thickness ratio t_0/t_1 and the initial imperfection were kept constant. It is observed that the adopted nondimensionalization of the variables is not totally adequate. This is due to the fact that the axial rigidity of the inside rings varies with R/t_1. For larger values of R/t_1 the effect of membrane forces and deformations is small in comparison to the bending ones. This effect increases for lower values of R/t_1. The major impact of the axial rigidity on the response occurs in the slope of the prebuckling path. For bigger R/t_1 values the initial slope is positive (see results for inextensional case in Kyriakides and Youn, 1984). For smaller R/t_1 values the initial slope is negative. In spite of these differences the limit pressure remains nearly proportional to $(R/t_1)^3$.

CONCLUSIONS

The paper addresses the problem of two concentric smoothly contacting rings under external pressure. The inner ring is initially partially detached from the outer one over a

small section. The problem was formulated through a "large deflection" set of kinematics and solved numerically. The solution procedure had to address the rather complex contact problem which develops between the two rings.

The presence of the outer ring has in general a stiffening effect on the response of the structure and leads to higher instability pressures. These characteristics are caused by the more complex equilibrium configurations to which the constrained inner ring must conform.

If the outer ring is relatively compliant (thin) the two rings deform in a doubly symmetric fashion similar to the one followed by an unconfined ring under external pressure. Beyond a certain deformation the composite structure experiences a substantial loss of stiffness but retains its load-bearing capacity.

When the relative stiffness of the outer ring is increased the response of the composite structure becomes stiffer but the nature of the instability changes to a limit load. As a result, beyond the limit load the structure loses a substantial part of its pressure-bearing capacity. The limit pressure is strongly related to the relative stiffness of the two rings and to the geometry of the initial imperfection. For even higher outer ring stiffnesses the preferred mode of deformation switches to one which has only one plane of symmetry.

The formulation and solution procedures presented can easily be modified to handle alternative loadings of the two rings and/or inelastic ring materials.

Acknowledgement—The work was carried out in part with support from the National Science Foundation under the PYI award MSM-8352370.

REFERENCES

Bottega, W. J. (1988). On the constrained elastic ring. *J. Engng Math.* **22**, 43–51.

Bucciarelli, L. L. and Pian, T. H. H. (1967). Effect of initial imperfections on the instability of a ring confined in an imperfect rigid boundary. *ASME J. Appl. Mech.* **89**, 979–984.

El-Bayoumi, L. (1972). Buckling of a circular elastic ring confined in a uniformly contracting circular cavity. *ASME J. Appl. Mech.* **94**, 758–766.

Kyriakides, S. (1986). Propagating buckles in long confined cylindrical shells. *Int. J. Solids Structures* **22**, 1579–1597.

Kyriakides, S. and Babcock, C. D. (1980). On the slip-on buckle arrestor for offshore pipelines. *ASME J. Pressure Vessel Tech.* **102**, 188–193.

Kyriakides, S. and Youn, S.-K. (1984). On the collapse of circular confined rings under external pressure. *Int. J. Solids Structures* **20**, 699–713.

Pian, T. H. H. and Bucciarelli, L. L. (1967). Buckling of radially constrained circular ring under distributed loading. *Int. J. Solids Structures* **3**, 715–730.

Powell, M. J. D. (1970). A hybrid method for nonlinear equations. In *Numerical Methods for Nonlinear Algebraic Equations* (Edited by P. Rabinowitz), Chapter 6. Gordon and Breach, New York.

Reissner, E. (1972). On one-dimensional finite-strain beam theory: the plane problem. *J. Appl. Math. Phys. (ZAMP)* **23**, 795–804.

Yamamoto, Y. and Matsubara, N. (1981). Buckling strength of steel cylindrical liners for waterway tunnels. *Theo. Appl. Mech.* (Japan) **30**, 225–235.

Zagustin, E. A. and Herrmann, G. (1967). Stability of an elastic ring in a rigid cavity. *ASME J. Appl. Mech.* **89**, 263–270.